Electrophysiology of
human cardiac atrial and ventricular telocytes

Jingwei Sheng [a], Winston Shim [a, b, *], Jun Lu [a], Sze Yun Lim [a], Boon Hean Ong [c], Tien Siang Lim [d], Reginald Liew [b], Yeow Leng Chua [c], Philip Wong [a, b, d]

[a] *Research and Development Unit, National Heart Centre Singapore, Singapore*
[b] *Duke-NUS, Graduate Medical School, Singapore*
[c] *Department of Cardiothoracic Surgery, National Heart Centre Singapore, Singapore*
[d] *Department of Cardiology, National Heart Centre Singapore, Singapore*

Abstract

Telocytes (TCs) with exceptionally long cellular processes of telopodes have been described in human epicardium to act as structural supporting cells in the heart. We examined myocardial chamber-specific TCs identified in atrial and ventricular fibroblast culture using immunocytochemistry and studied their electrophysiological property by whole-cell patch clamp. Atrial and ventricular TCs with extended telopodes and alternating podoms and podomers that expressed CD34, c-Kit and PDGFR-β were identified. These cells expressed large conductance Ca^{2+}-activated K^+ current (BK_{Ca}) and inwardly rectifying K^+ current (IK_{ir}), but not transient outward K^+ current (I_{to}) and ATP-sensitive potassium current (K_{ATP}). The active channels were functionally competent with demonstrated modulatory response to H_2S and transforming growth factor (TGF)-β1 whereby H_2S significantly inhibited the stimulatory effect of TGF-β1 on current density of both BK_{Ca} and IK_{ir}. Furthermore, H_2S attenuated TGF-β1-stimulated KCa1.1/Kv1.1 (encode BK_{Ca}) and Kir2.1 (encode IK_{ir}) expression in TCs. Our results show that functionally competent K^+ channels are present in human atrial and ventricular TCs and their modulation may have significant implications in myocardial physiopathology.

Keywords: Telocyte ● potassium channel ● hydrogen sulphide ● fibrosis

Introduction

Telocytes (TC) are newly identified cells that are found in the interstitial space of many organs, including heart [1], bladder [2], lungs [3] and skeletal muscle [4] and intimately contacting the parenchymal tissues. They have previously been described as interstitial Cajal-like cells in atrial and ventricular myocardium [5, 6] and very little was known of their function. Recently, TCs have been increasingly recognized to play key supporting physiological roles in the heart because of the seminal work of Popescu and colleagues [7–9]. Telocytes have exceptionally long (10–1000 μm), moniliform cellular processes named telopodes (Tps) with intervening podoms and podomers that form an interstitial network connecting different segments of the heart [10] including those of the epicardium [11, 12], myocardium [8, 13] and endocardium [14]. Their close physical association with cardiac progenitors and cardiomyocytes in the stem cell niche has been suggested to be important in the repair and regeneration of infarcted myocardium [11].

Recently, human myometrial TCs have been reported to express calcium-dependent hyperpolarization-activated chloride inward current [15]. However, very limited is known about the electrophysiological activity of cardiac TCs although they have been suggested to act as intercellular signalling intermediary in the myocardium with potential role in cardiac rhythm [11] and atrial fibrillation [16]. We have recently showed that hydrogen sulphide (H_2S) modulated the activity of ion channels in human atrial fibroblasts and suppressed their transformation into myofibroblasts in response to transforming growth factor (TGF)-β1. This may have important implications in TGF-β1-mediated cardiac fibrosis and its associated atrial fibrillation [17]. In this study, we present first evidence of electrophysiological properties of human TCs derived from atrial and ventricular myocardium and demonstrate the modulatory role of H_2S on the ion channel activity.

*Correspondence to: Winston SHIM,
Research and Development Unit, National Heart Centre, 9 Hospital Drive, School of Nursing, #03-02, Block C, Sing Health Research Facilities, 169612, Singapore.
Tel.: 65 6435 0752
Fax: 65 6226 3972
E-mail: winston.shim.sn@nhcs.com.sg

Materials and methods

Telocyte identification

Informed consent was gathered from male patients ($n = 10$) with mean age of 63 ± 8.7 years old who were scheduled for coronary bypass surgery and were hyperlipidemic, managed with anti-hypertensive and diabetic medications. The protocol was approved by institutional review board of Singapore General Hospital that conformed to the Declaration of Helsinki. Atrial appendages were collected as surgical by-product. Human atrial interstitial cells were isolated by mincing the appendages to less than 1 mm^3 and followed by 0.1% trypsin digestion for 20 min. before plating onto tissue culture-treated 60-mm dishes to produce fibroblastic outgrowth from minced tissue pieces. Outgrown fibroblasts were harvested and re-plated onto a fresh tissue culture dish as passage 1 to isolate homogeneous fibroblast culture that expressed collagen I and fibroblast marker as described previously by our group [18]. Atrial fibroblasts were passaged as monolayer in 10% foetal bovine serum supplemented DMEM and antibiotics (100 U/ml penicillin G and 100 μg/ml streptomycin) at 37°C in a humidified atmosphere of 95% air and 5% CO_2. Human cardiac ventricular fibroblasts (cat no. CC-2904) were acquired from Lonza Inc (Singapore). These cells were isolated from normal adult heart and certified to express greater than 90% collagen I and negative for von Willebrand factor VIII-related antigen. After 3 passages of the atrial and ventricular culture, TCs were distinguishable from other interstitial cells and were typically identified by their characteristic ultra-long moniliform cellular processes of Tps under light microscopy and the cultures from passages 3 to 5 were used for subsequent experiments. These TCs containing cultures were seeded on glass coverslips for immunostaining or in 35 mm dish for whole-cell patch-clamp recordings.

Immunocytochemistry/Immunohistochemistry

Telocytes were cultured on coverslips, were fixed with 2% paraformaldehyde/PBS for 15 min., permeabilized by 20 min. incubation in PBS containing 0.1% Triton X-100, and blocked in PBS containing 2.5% bovine serum albumin (BSA). Samples were then incubated overnight at 4°C with primary antibodies in PBS containing 0.1% BSA, after which they were incubated for 1 hr at room temperature with secondary antibody. Coverslips were rinsed and mounted on glass slides and examined by using confocal microscopy. Primary antibodies against CD34 (1:10; BD Biosciences, San Jose, CA, USA), c-Kit (1:200; Novus Biologicals, Littleton, CO, USA) and PDGF receptor (PDGFR)-β (1:1000; Cell Signaling, Danvers, MA, USA) were used to identify TCs. Primary antibodies used were anti-Kv1.1 (1/1000; Abcam, Cambridge, MA, USA) to label BK_{Ca} channels, anti-Kv4.3 (1/500; Abcam) to label I_{to} channels and anti-Kir2.1 (1/1000; Abcam) to label IK_{ir} channels. Secondary antibodies used were Alexa Fluor555 (1/1000) and Alexa Fluor488 (1/500)-labelled antibodies (Life Technologies, Carlsbad, CA, USA). Counter staining was performed using DAPI (4′, 6-diamidino-2-phenylindole) to visualize nuclei.

Electrophysiological recordings

Cell were placed on the stage of a Nikon Diaphot inverted microscope and superfused continuously at 36 ± 1°C with Tyrode solution containing (in mM) 140 NaCl, 5.4 KCl, 1.8 $CaCl_2$, 1 $MgCl_2$, 10 HEPES and 10 Glucose (pH adjusted to 7.4 with NaOH). The patch-clamped cell was superfused by means of a temperature-controlled micro-superfusor (TC-324B; Warner Instruments, Hamden, CT, USA). Patch pipettes were made from borosilicate glass shanks (Sutter Instrument, Novato, CA, USA) and pulled with a Brown–Flaming puller (Model P-97; Sutter Instrument Co), and had tip resistances of 2–3 MΩ when filled with pipette solution. Pipette tips were polished (Microforge MF830; Narishige, Tokyo, Japan). The patch pipettes were filled with a standard solution containing (in mM) 140 KCl, 1.2 $MgCl_2$, 0.05 EGTA, 10 HEPES, 0.1 GTP and 5.0 Mg ATP (pH adjusted to 7.2 with KOH). After a gigaohm seal was obtained by negative pressure suction, the cell membrane was ruptured by a gentle suction to establish whole-cell configuration with a seal resistance >800 MΩ. The cell membrane capacitance (40.3 ± 8.2 pF) was electrically compensated with the pulse software. The series resistance (Rs, 3–5 MΩ) was compensated by 50–70% to minimize voltage errors. Currents were elicited with voltage protocols as described in the following results section for different individual current recordings. Whole-cell voltage-clamp experiments were performed with an Axopatch 200B amplifier (Axon Instruments, Foster City, CA, USA) interfaced to a Digidata 1322A data acquisition system controlled by Clampex version 8.1 software (Axon Instruments). Data were analysed with pCLAMP software (Version 10.0; Axon Instrument) and Origin 8.0 (OriginLab, Northampton, MA, USA).

Statistical analysis

All data were presented as mean $\pm$ SE. Statistical significance of the difference between groups was determined using Student's t-test as appropriate. A value of $P < 0.05$ was considered statistically significant.

Results

Identification of cardiac telocytes

Telocytes were clearly identifiable in our human atrial and ventricular cardiac fibroblast culture by phase contrast after passage 3. Telocytes displayed characteristic long Tps (100–500 μm) [9] with occasional podomers and podoms that were often in contact with fibroblasts and other TCs [19]. In accordance with previous reports [1, 8, 20], these human TCs stained positive for CD34, c-Kit (CD34/c-Kit double staining in Fig. S1) and PDGFR-β markers (Fig. 1).

Ion currents in human atrial and ventricular telocytes

To record and characterize ion currents in single TCs, cells with long Tps were selected under light microscopy with patch pipettes (Fig. 2) and conventional whole-cell voltage-clamp experiment was performed at 36 ± 0.5°C. Outward currents were activated at depolarization voltages between -30 mV and $+90$ mV in 10 mV increments from a holding potential of -40 mV. Compared to baseline current density (8.3 ± 2.8 pA/pF, $n = 6$ atrial TCs; 8.9 ± 2.1 pA/pF, $n = 6$ ventricular TCs), the activated currents were sensitive to inhibition
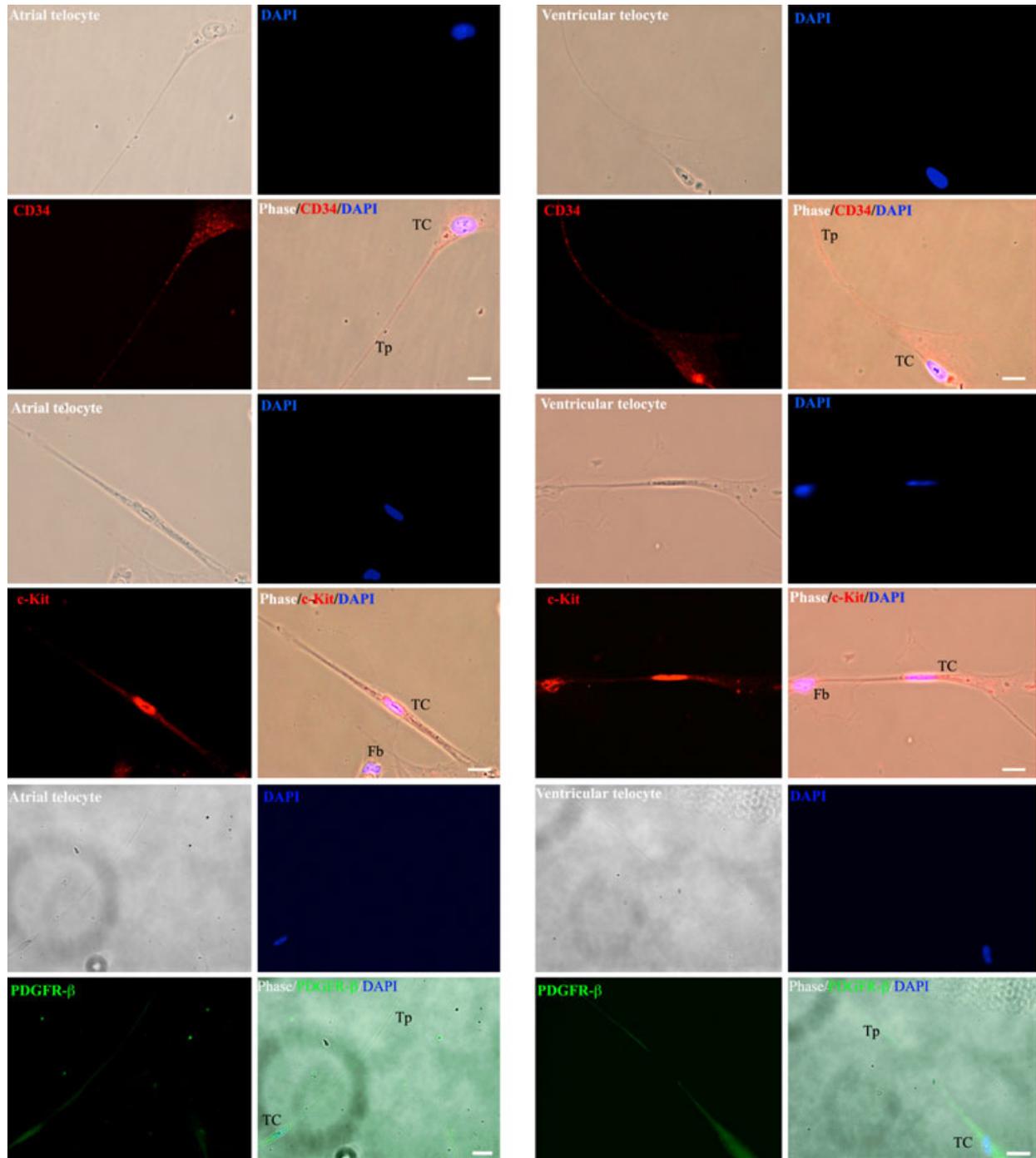
Fig. 1 Identification of cardiac atrial and ventricular telocytes (TCs). Immunofluorescent staining for anti-CD34 (red), c-kit (red) and vimentin (green) demonstrated cells with very small cell bodies (~1:1 ratio cytoplasm to nucleus) and extremely long and thin cellular processes of telopode (Tp) scattered among atrial and ventricular fibroblasts (Fb). TC: telocyte; Fb: cardiac fibroblast; Tp: telopode. Scale bar corresponds to 10 μm.

$(1.8 \pm 0.4$ pA/pF, $P < 0.01$, $n = 6$ atrial TCs; 2.3 ± 0.5 pA/pF, $P < 0.01$, $n = 6$ ventricular TCs) at +90 mV by 1 mM Paxilline (a specific BK_{Ca} inhibitor) and were responsive (32.4 ± 3.1 pA/pF,

$P < 0.01$, $n = 6$ atrial TCs; 20.9 ± 4.2 pA/pF, $P < 0.01$, $n = 6$ ventricular TCs) at +90 mV to stimulation by 10 μM (+/−) Naringenin (a specific BK_{Ca} opener), confirming the presence of BK_{Ca} currents in
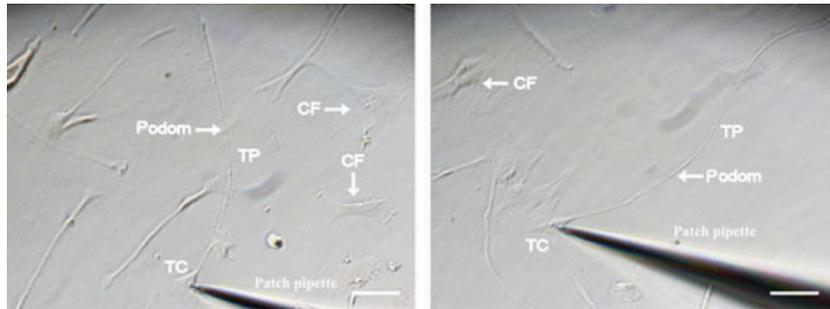
Fig. 2 Photomicrographs showing atrial (left) and ventricular (right) telocytes before patch clamping was attempted. TC: telocyte; Fb/CF: cardiac fibroblast; Tp: telopode. Scale bar corresponds to 50 μm.
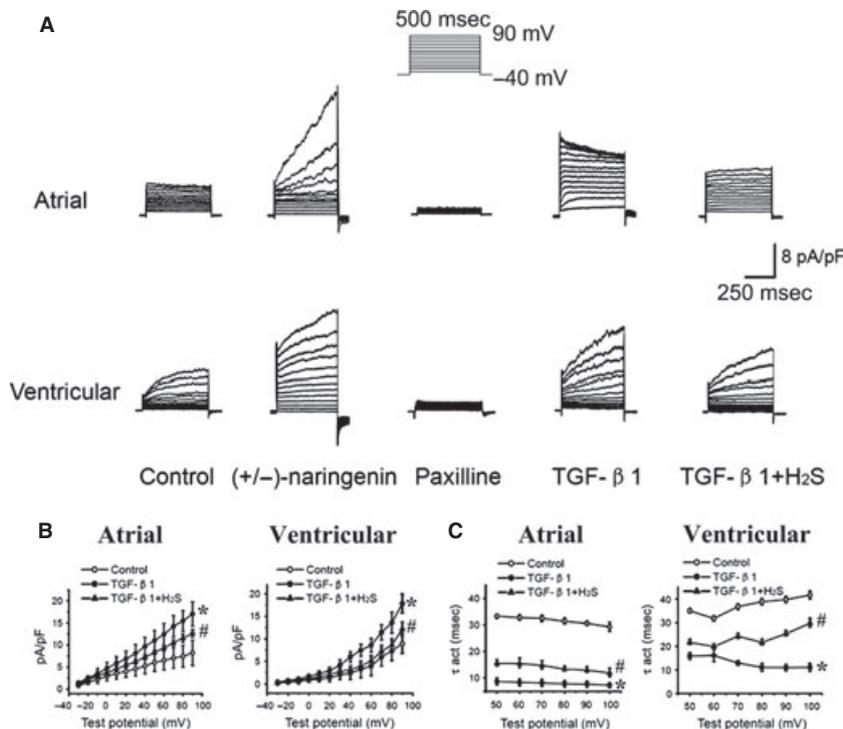

Fig. 3 BK_{Ca} currents in human atrial and ventricular telocytes. (**A**) voltage-dependent current was changed by BK_{Ca} specific blocker Paxilline (100 μM) and opener Naringenin (10 μM) respectively. Effect of H_2S (100 μM) on BK_{Ca} currents in the presence of transforming growth factor (TGF)-β1 (1 ng/ml). (**B**) Mean I–V relationship for peak BK_{Ca} in the absence and presence of H_2S (100 μM) and TGF-β1 (1 ng/ml; *$P < 0.05$ *versus* basal levels. #$P < 0.05$ *versus* TGF-β1 alone; $n = 6$). (**C**) Plot of the activation τ (τ_{act}) as a function of membrane potential in the presence of TGF-β1 (1 ng/ml) before H_2S (100 μM) addition (*$P < 0.05$ *versus* basal levels. #$P < 0.05$ *versus* TGF-β1 alone; $n = 6$).

atrial and ventricular TCs (Fig. 3A). Furthermore, under identical voltage-clamp condition, 1 ng/ml TGF-β1 significantly increased the peak BK_{Ca} current density (17.1 ± 2.7 pA/pF, $P < 0.01$, $n = 6$ atrial TCs; 17.8 ± 2.1 pA/pF, $P < 0.05$, $n = 6$ ventricular TCs) at +90 mV. However, additional presence of H_2S (100 μM) reduced the effect of TGF-β1 (12.6 ± 0.8 pA/pF, $P < 0.05$, $n = 6$ atrial TCs; 12.2 ± 1.6 pA/pF, $P < 0.05$, $n = 6$ ventricular TCs), thereby demonstrating functionality of the channels and confirming the inhibitory effect of H_2S on BK_{Ca} currents in TCs (Fig. 3B). Moreover, the rising phase of BK_{Ca} currents at +100 mV with activation τ (τ_{act}) at baseline (29.3 ± 1.7 ms, atrial TCs; 41.6 ± 1.6 ms, ventricular TCs) was lowered significantly by TGF-β1 (7.3 ± 0.7 ms, $P < 0.05$, $n = 6$ atrial TCs; 11.1 ± 0.1 ms, $P < 0.05$, $n = 6$ ventricular TCs), but was significantly reversed (11.9 ± 0.3 ms, $P < 0.05$, $n = 6$ atrial TCs; 29.1 ± 0.3 ms, $P < 0.05$, $n = 6$ ventricular TCs) by H_2S, confirming its modulation of BK_{Ca} channel kinetics in TCs (Fig. 3C).

Similarly, under conditions that elicited total outward K^+ currents, it was found that the activated currents were insensitive to 4-aminopyridine (4-AP; 0.5 mM) inhibition, indicating the absence of transient outward currents (I_{to}) in atrial and ventricular TCs (Fig. 4A). Furthermore, currents elicited from the holding potential of −40 mV that ramped every 9 sec. from −120 mV to +60 mV at 20 mV/sec. and subsequently ramped to −40 mV at −100 mV/sec. were not responsive to 30 μM pinacidil (K_{ATP} specific channel enhancer), suggesting ATP-sensitive K current (K_{ATP}) was not present in atrial and ventricular TCs (Fig. 4B). Such differential ion channel profile of TCs further differentiated them from cardiac fibroblasts that showed higher BK_{Ca} current density and presence of I_{to} and K_{ATP} currents that were previously reported by our group [18].

Next, we elicited inwardly rectifying K^+ currents by depolarizing the TCs with a 2 sec. ramp protocol of −120 to 0 mV from holding potential of −40 mV. Similar to our previous report of IK_{ir} current in
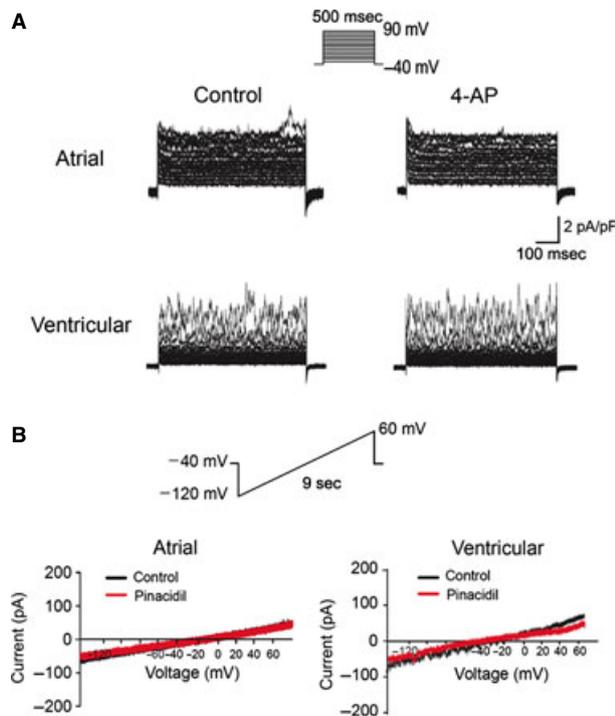
Fig. 4 I_{to} and K_{ATP} currents are not detectable in human atrial and ventricular telocytes. (**A**) Effect of I_{to} inhibitor 4-AP (5 mM) on membrane currents in human atrial and ventricular telocytes showing no noticeable inhibition. (**B**) Effect of K_{ATP} specific opener Pinacidil on currents elicited by the voltage protocol showing no appreciable enhancement in amplitude.

human atrial fibroblasts that was attenuated by Ba^{2+} ion [18], addition of Ba^{2+} attenuated the inwardly rectifying currents in both atrial and ventricular TCs, and a 20 mM K^+ in the bath solution induced a strong increase in the current amplitude, confirming the presence of IK_{ir} inward current in TCs (Fig. 5A). Furthermore, slope conductance [21] of IK_{ir} in atrial and ventricular TCs were 9.5 $\pm$ 4.1 pS/pF ($n = 6$) and 3.1 $\pm$ 1.2 pS/pF ($n = 6$) in 5.4 mmol/l $[K]_o$ respectively. The baseline current density of IK_{ir} at -120 mV (-4.3 ± 0.4 pA/pF, atrial TCs; -4.1 ± 0.3 pA/pF, ventricular TCs) was increased by 1 ng/ml TGF-β1 (-6.4 ± 0.1 pA/pF, $P < 0.01$, $n = 6$ atrial TCs; -5.2 ± 0.1 pA/pF, $P < 0.01$, $n = 6$ ventricular TCs), confirming the functionality of IK_{ir} channel. However, the current density at -120 mV reverted towards baseline (-5.8 ± 0.3 pA/pF, $P < 0.05$, $n = 6$ atrial TCs; -4.3 ± 0.3 pA/pF, $P < 0.05$, $n = 6$ ventricular TCs) in the presence of H_2S (Fig. 5B).

H_2S attenuated TGF-β1-induced KCa1.1 and Kir2.1 expression in cardiac telocytes

Transforming growth factor-β1 is a major mediator of myocardial fibrosis. Our previous study showed that exogenously applied H_2S significantly attenuated TGF-β1-stimulated KCa1.1/Kv1.1 (responsible for BK_{Ca}) and Kir2.1 (responsible for IK_{ir}) expression and reduced proliferation of human atrial fibroblasts [18]. Consistent with our elec-

trophysiological findings, immunofluorescent staining with anti-Kv1.1 and anti-Kir2.1 antibodies confirmed their presence in cardiac TCs (Fig. 6). Furthermore, stimulation with TGF-β1 enhanced the channel expression in cardiac fibroblasts, but also in the associated TCs. Similarly, pretreatment with H_2S for 24 hrs reduced the expression levels and organizational distribution of Kv1.1 and Kir2.1 induced by TGF-β1, supporting its inhibitory role on channel expression in cardiac TCs. Contrary to atrial fibroblasts [22] and cardiac fibroblasts in this study, Kv4.3 (responsible for I_{to}) expression in TCs was barely above background noise levels (data not shown), which supported the undetectable I_{to} current in our electrophysiological findings.

Discussion

Telocytes have previously been reported in human epicardium [1]. Our results confirmed that ionic active cardiac TCs are present in the human atrial and ventricular myocardium. Concordance with previous report [23], they expressed c-Kit, CD34 and PDGFR-β [20] and exhibited typical TC phenotype such as Tps, podoms and podomers [19]. Because of these unique structural characteristics, TCs with moniliform processes were relatively straightforward to distinguish from cultured fibroblasts and other interstitial cells that maintained disparate spindle-like and stellate-shaped cells in culture. On the basis of these criteria, we were able to visually isolate single TCs from human atrial and ventricular fibroblasts and other interstitial cells for their electrophysiological studies. The examined cardiac TCs expressed a subset of ionic currents that was previously reported to be present in human atrial fibroblasts [18]. To our knowledge, this is the first study that provides evidence of BK_{Ca} and IK_{ir} channels and functionally active currents in human atrial and ventricular TCs.

To date, only very limited is known about the electrophysiological property of isolated TCs. In human myometrium, patch-clamp recordings of TCs revealed a calcium-dependent hyperpolarization-activated chloride inward current, but absence of L-type calcium channels, which was postulated to modulate myometrial smooth muscle contractions [15]. Inwardly rectifying chloride current has been identified in rodent interstitial cells of Cajal (ICC) in regulating gut pacemaker activity [24]. Transient outward potassium current that modulated pacemaker potential has also been described in rodent ICC [25]. Although transient outward I_{to} and ATP-sensitive K_{ATP} currents were not detected in both the atrial and ventricular TCs in this study, the presence of functionally active BK_{Ca} and hyperpolarized-activated inwardly rectifying IK_{ir} channels and their close proximity to cardiac fibroblasts and cardiomyocytes may suggest a probable role of cardiac TCs within the multicellular framework that facilitates mechano-electrical coupling of the heart.

Myofibroblasts are abundant in fibrosis [26] and have been associated with TGF-β1- mediated atrial fibrillation in rodent [27] and in patients with inflammation-linked atrial remodelling [17]. Preventing aberrant proliferation of cardiac fibroblasts and their transformation to myofibroblasts has been an attractive target in limiting fibrosis. Our previous study showed that H_2S effectively suppressed proliferation of atrial fibroblasts by inhibiting BK_{Ca}, IK_{ir} and I_{to} channels [18]. Consistently, we found that H_2S attenuated TGF-β1-induced BK_{Ca}

© 2014 The Authors.

359

Journal of Cellular and Molecular Medicine published by John Wiley & Sons Ltd and Foundation for Cellular and Molecular Medicine.
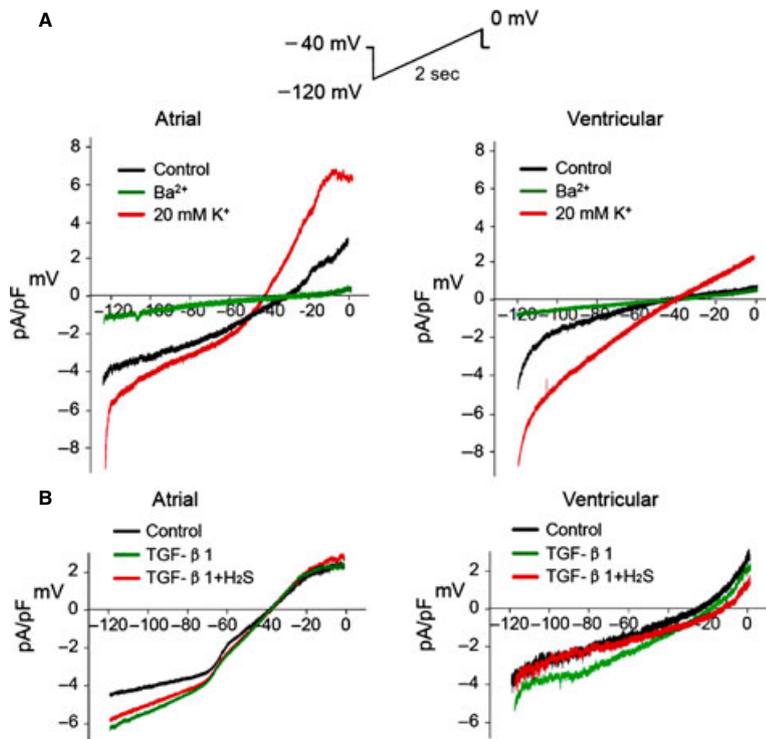
Fig. 5 I_{Kir} in human atrial and ventricular telocytes. (**A**) Effect of Ba^{2+} on membrane current in human atrial and ventricular telocytes. Representative I–V relationships of membrane currents recorded with a 2-sec. ramp protocol (-120 to 0 mV from a holding potential of -40 mV) in 5 mM K^+ or 20 mM K^+ and after application of 0.5 mM Ba^{2+}. (**B**) Effect of H_2S (100 μM) on I_{Kir} currents in the presence of transforming growth factor-β1 (1 ng/ml) in human atrial and ventricular telocytes.
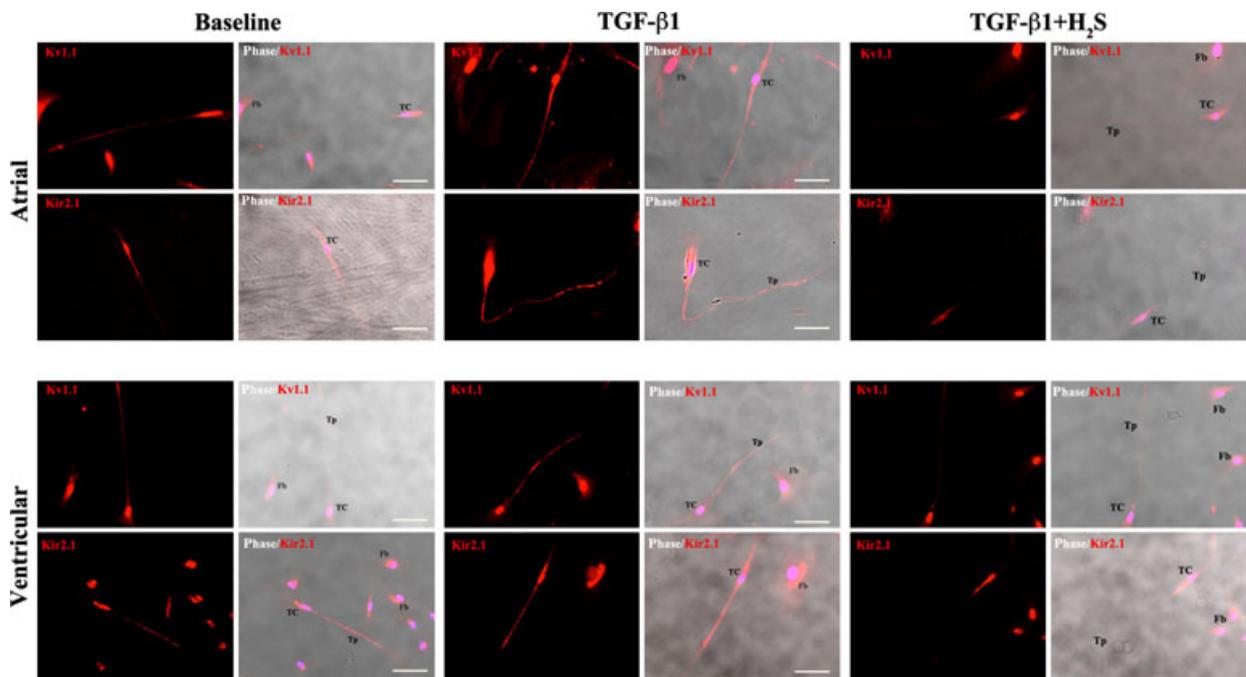

Fig. 6 Immunostaining of BK_{Ca} (Kv1.1) and IK_{ir} (Kir2.1) in human atrial (top) and ventricular (bottom) telocytes. Cells were stained with anti-Kv1.1 (red), anti-Kir2.1 (red) and the nuclei were stained using DAPI (blue). H_2S attenuates the Kv1.1 and Kir2.1 upregulation induced by transforming growth factor-β1. TC: telocyte; Fb: cardiac fibroblast; Tp: telopode. Scale bar corresponds to 50 μm.

activation and decelerated the transition from closed to open state of the channel, suggesting a role for H_2S in regulating BK_{Ca} channel kinetic and voltage sensitivity in human cardiac TCs. Furthermore, H_2S down-regulated the voltage-dependent relationships of IK_{ir} induced by TGF-β1 in the TCs. It is currently unclear about the implications of greater BK_{Ca} (Fig. 3C) and IK_{ir} (Fig. 5B) channel responsiveness observed in the atrial TCs as compared to ventricular TCs when stimulated with TGF-β1. This was despite both TCs exhibited similar current density of BK_{Ca} (Fig. 3B) and IK_{ir} (Fig. 5A) at baseline. Although atrial fibroblasts are known to participate more actively in cardiac fibrosis as compared to ventricular fibroblasts [28, 29], it remains to be ascertained if such differential sensitivity of atrial TCs to TGF-β1 stimulation has a role in more aggressive fibrotic response of atrial fibroblasts. Furthermore, the differential disease status of the atrial and ventricular tissue donors (from which TCs were derived in our study), in affecting the observed outcome could not be totally discounted.

In summary, our study shows the presence of functionally competent BK_{Ca} and IK_{ir} channels, but not I_{to} and K_{ATP} channels, in cardiac atrial and ventricular TCs. Their close physical association with cardiac fibroblasts and cardiomyocytes may suggest additional active roles in myocardial physiopathology apart from mere passive structural supporting function in the heart.

Funding

Conflict of interest

The authors confirm that there are no conflicts of interest.

Supporting information

Additional Supporting Information may be found in the online version of this article:

Figure S1 Double immunofluorescent staining of human atrial and ventricular telocytes demonstrating positivity for CD34 and c-Kit. Scale bar corresponds to 10 μm.

References

1. **Popescu LM, Manole CG, Gherghiceanu M, et al.** Telocytes in human epicardium. *J Cell Mol Med.* 2010; 14: 2085–93.

2. **Parajuli SP, Soder RP, Hristov KL, et al.** Pharmacological activation of small conductance calcium-activated potassium channels with naphtho[1,2-d]thiazol-2-yl-amine decreases guinea pig detrusor smooth muscle excitability and contractility. *J Pharmacol Exp Ther.* 2012; 340: 114–23.

3. **Zheng Y, Li H, Manole CG, et al.** Telocytes in trachea and lungs. *J Cell Mol Med.* 2011; 15: 2262–8.

4. **Popescu LM, Manole E, Serboiu CS, et al.** Identification of telocytes in skeletal muscle interstitium: implication for muscle regeneration. *J Cell Mol Med.* 2011; 15: 1379–92.

5. **Hinescu ME, Gherghiceanu M, Mandache E, et al.** Interstitial Cajal-like cells (ICLC) in atrial myocardium: ultrastructural and immunohistochemical characterization. *J Cell Mol Med.* 2006; 10: 243–57.

6. **Hinescu ME.** Popescu LM Interstitial Cajal-like cells (ICLC) in human atrial myocardium. *J Cell Mol Med.* 2005; 9: 972–5.

7. **Gherghiceanu M, Popescu LM.** Heterocellular communication in the heart: electron tomography of telocyte-myocyte junctions. *J Cell Mol Med.* 2011; 15: 1005–11.

8. **Bani D, Formigli L, Gherghiceanu M, et al.** Telocytes as supporting cells for myocar-dial tissue organization in developing and adult heart. *J Cell Mol Med.* 2010; 14: 2531–8.

9. **Popescu LM.** Faussone-Pellegrini MS TELO-CYTES - a case of serendipity: the winding way from Interstitial Cells of Cajal (ICC), *via* Interstitial Cajal-Like Cells (ICLC) to TELOCYTES. *J Cell Mol Med.* 2010; 14: 729–40.

10. **Gherghiceanu M, Popescu LM.** Cardiac telocytes - their junctions and functional implications. *Cell Tissue Res.* 2012; 348: 265–79.

11. **Popescu LM, Gherghiceanu M, Manole CG, et al.** Cardiac renewing: interstitial Cajal-like cells nurse cardiomyocyte progenitors in epicardial stem cell niches. *J Cell Mol Med.* 2009; 13: 866–86.

12. **Gittenberger-de Groot AC, Winter EM, Poel-mann RE.** Epicardium-derived cells (EPDCs) in development, cardiac disease and repair of ischemia. *J Cell Mol Med.* 2010; 14: 1056–60.

13. **Kostin S.** Myocardial telocytes: a specific new cellular entity. *J Cell Mol Med.* 2010; 14: 1917–21.

14. **Gherghiceanu M, Manole CG, Popescu LM.** Telocytes in endocardium: electron microscope evidence. *J Cell Mol Med.* 2010; 14: 2330–4.

15. **Cretoiu SM, Cretoiu D, Marin A, et al.** Telocytes: ultrastructural, immunohistochemical and electrophysiological characteristics in human myometrium. *Reproduction.* 2013; 145: 357–70.

16. **Kostin S, Popescu LM.** A distinct type of cell in myocardium: interstitial Cajal-like cells (ICLCs). *J Cell Mol Med.* 2009; 13: 295–308.

17. **Mira YE, Muhuyati, Lu WH, et al.** TGF-beta1 signal pathway in the regulation of inflammation in patients with atrial fibrillation. *Asian Pac J Trop Med.* 2013; 6: 999–1003.

18. **Sheng J, Shim W, Wei H, et al.** Hydrogen sulphide suppresses human atrial fibroblast proliferation and transformation to myofi-broblasts. *J Cell Mol Med.* 2013; 17: 1345–54.

19. **Mou Y, Wang Y, Li J, et al.** Immunohisto-chemical characterization and functional identification of mammary gland telocytes in the self-assembly of reconstituted breast cancer tissue *in vitro. J Cell Mol Med.* 2013; 17: 65–75.

20. **Xiao J, Wang F, Liu Z, et al.** Telocytes in liver: electron microscopic and immunofluo-rescent evidence. *J Cell Mol Med.* 2013; 17: 1537–42.

21. **Schubert R, Krien U, Wulfsen I, et al.** Nitric oxide donor sodium nitroprusside dilates rat small arteries by activation of inward recti-fier potassium channels. *Hypertension.* 2004; 43: 891–6.

22. **Sheng J, Shim W, Wei H, *et al.*** Hydrogen sulphide suppresses human atrial fibroblast proliferation and transformation to myofibroblasts. *J Cell Mol Med.* 2013; 17: 1345–54.

23. **Zhao B, Chen S, Liu J, *et al.*** Cardiac telocytes were decreased during myocardial infarction and their therapeutic effects for ischaemic heart in rat. *J Cell Mol Med.* 2013; 17: 123–33.

24. **Zhu Y, Mucci A, Huizinga JD.** Inwardly rectifying chloride channel activity in intestinal pacemaker cells. *Am J Physiol Gastrointest Liver Physiol.* 2005; 288: G809–21.

25. **Parsons SP, Huizinga JD.** Transient outward potassium current in ICC. *Am J Physiol Gastrointest Liver Physiol.* 2010; 298: G456–66.

26. **Guo W, Shan B, Klingsberg RC, *et al.*** Abrogation of TGF-beta1-induced fibroblast-myofibroblast differentiation by histone deacetylase inhibition. *Am J Physiol Lung Cell Mol Physiol.* 2009; 297: L864–70.

27. **Choi EK, Chang PC, Lee YS, *et al.*** Triggered firing and atrial fibrillation in transgenic mice with selective atrial fibrosis induced by over-expression of TGF-beta1. *Circ J.* 2012; 76: 1354–62.

28. **Hanna N, Cardin S, Leung TK, *et al.*** Differences in atrial *versus* ventricular remodeling in dogs with ventricular tachypacing-induced congestive heart failure. *Cardiovasc Res.* 2004; 63: 236–44.

29. **Burstein B, Libby E, Calderone A, *et al.*** Differential behaviors of atrial *versus* ventricular fibroblasts: a potential role for platelet-derived growth factor in atrial-ventricular remodeling differences. *Circulation.* 2008; 117: 1630–41.